

Absorption and attenuation of visible and near-infrared light in water: dependence on temperature and salinity

W. Scott Pegau, Deric Gray, and J. Ronald V. Zaneveld

We have measured the absorption coefficient of pure and salt water at 15 wavelengths in the visible and near-infrared regions of the spectrum using WETLabs nine-wavelength absorption and attenuation meters and a three-wavelength absorption meter. The water temperature was varied between 15 and 30 °C, and the salinity was varied between 0 and 38 PSU to study the effects of these parameters on the absorption coefficient of liquid water. In the near-infrared portion of the spectrum the absorption coefficient of water was confirmed to be highly dependent on temperature. In the visible region the temperature dependence was found to be less than $0.001 \text{ m}^{-1}/^{\circ}\text{C}$ except for a small region around 610 nm. The same results were found for the temperature dependence of a saltwater solution. After accounting for index-of-refraction effects, the salinity dependence at visible wavelengths is negligible. Salinity does appear to be important in determining the absorption coefficient of water in the near-infrared region. At 715 nm, for example, the salinity dependence was $-0.00027 \text{ m}^{-1}/\text{PSU}$. Field measurements support the temperature and salinity dependencies found in the laboratory both in the near infrared and at shorter wavelengths. To make estimates of the temperature dependence in wavelength regions for which we did not make measurements we used a series of Gaussian curves that were fit to the absorption spectrum in the visible region of the spectrum. The spectral dependence on temperature was then estimated based on multiplying the Gaussians by a fitting factor. © 1997 Optical Society of America

Key words: Absorption, water, temperature, salinity.

1. Introduction

The optical properties of liquid water are the basic building blocks on which hydrologic optics is built. To understand the optical properties of the oceans we must understand the optical properties of liquid water, which is the major component of the oceans. The two major mechanisms by which light interacts with water are scattering and absorption. Scattering by water has been studied both theoretically and experimentally. Although there are some differences in the estimates of scattering by pure water¹ the connection between theory and experiment is well developed.² In contrast, our theoretical and experimental understanding of absorption by water is quite

limited. The lack of agreement on the structure of liquid water³ hampers the task of solving Schrödinger's equation, from which we might be able to get a theoretical handle on absorption.

Measurement of the absorption coefficient in the visible region (400–700 nm) is difficult because of the low absorption values in this region. Contaminants in the water, such as dissolved organics, also interfere with accurate measurements in the visible region. An illustration of the difficulties in measuring the absorption coefficient of pure water is provided in Fig. 1. The variability of the measured absorption coefficients in the near-ultraviolet and blue portions of the spectrum are most likely due to the presence of contaminants. Some of this variability might conceivably be explained by the absorption coefficient of water being dependent on temperature. The possible temperature dependence^{1,4,5} throughout the visible portion of the spectrum was not examined in the investigations shown in Fig. 1. The possibility that the temperature effects contributed significantly to the variability evident in Fig. 1 was a motivating force for this study.

The authors are with the College of Oceanic and Atmospheric Sciences, Oregon State University, 104 Oceanic Administration Building, Corvallis, Oregon 97331.

Received 10 July 1996; revised manuscript received 13 January 1997.

0003-6935/97/246035-12\$10.00/0

© 1997 Optical Society of America

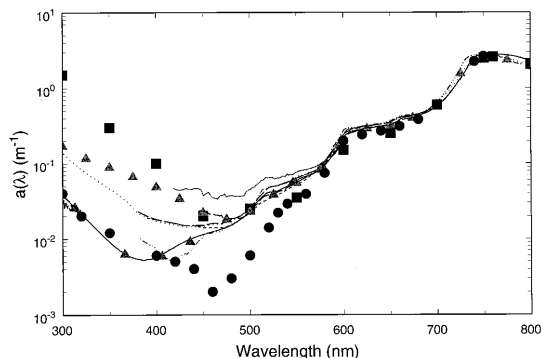


Fig. 1. Absorption coefficient of pure water as measured or compiled by several investigators.^{1,2,11,18,19,21,26-33} The discrepancy in the estimated absorption coefficients is largest at short wavelengths where absorption by organic contaminants is significant. At wavelengths longer than 550 nm the standard deviation of the estimates is between 5 and 10% of the mean value.

The effects of temperature and salinity are also important in the operation of instruments in which pure water is used as a reference medium.^{4,6} Such instruments include dual-beam spectrophotometers and the nine-wavelength absorption and attenuation meter (ac-9). These instruments are used to measure the absorption coefficient of samples that may have a different temperature or salinity than the reference water. Such differences occur when saline, cold natural samples are referenced against a freshwater blank that is typically laboratory temperature. It has been shown that in the near-infrared region of the spectrum an apparently negative absorption by dissolved materials may be observed if the temperature difference is not accounted for.⁷ *In situ* measurements, with systems like the ac-9, are made at ambient temperatures and salinities. The effect of temperature and salinity on absorption must then be known to interpret the measured absorption values. Not accounting for the change in the absorption coefficient with temperature or salinity, in laboratory or field measurements, could lead to errors in the measurement of absorption by colored dissolved organic matter by creating errors in the baseline, which have been seen to exist.^{7,8} Measurements of other optical properties, such as remotely sensed reflectance, which depend on the inherent optical properties of water, must also account for the possible effects of temperature and salinity.⁴

Despite the importance of water in oceanographic studies, the dependence of the absorption coefficient of water on temperature and salinity has not been definitively determined. Højerslev and Trabjerg⁴ stimulated the recent interest in the effect of environmental conditions on the absorption coefficient of water. Their work has led to further investigations of the role of temperature on the absorption coefficient of water^{1,5,7,9} including this study. Three of the studies^{1,4,5} found a constant temperature dependence of the order of $0.001 \text{ m}^{-1}/^{\circ}\text{C}$ within the blue-green portion of the spectrum. In contrast with earlier studies^{1,4} Trabjerg and Højerslev⁵ recently found the

absorption coefficient to decrease with increasing temperature ($\sim -0.001 \text{ m}^{-1}/^{\circ}\text{C}$) throughout the visible part of the spectrum. In our earlier study⁷ we were unable to discern such a dependence, and that investigation focused on the change in shape of the absorption spectrum with changing temperature. The constant temperature dependence was not observed in our preliminary study using an ac-9.⁹ Here we use an increased number of wavelengths and more stable instrumentation to follow up on our preliminary laboratory work.

As was the case with temperature there has been little research done in studying the role of salinity on the optical properties of water at visible wavelengths.^{10,11} This study spans the wavelength regions covered in the previous studies to provide a more comprehensive understanding of the effects of dissolved salt on the absorption coefficient. By changing the concentration of salt incrementally we show how the absorption coefficient depends on salinity over a wide range of naturally occurring salinities.

The absorption coefficient of water has been shown to be dependent on temperature at the overtones of the O-H vibrational frequencies in the infrared and near-infrared portions of the spectrum.^{7,12-14} The absorption by water in the same spectral bands has also been shown to depend on salinity.^{11,15} Here we use laboratory and field measurements to extend the investigation of the effects of temperature and salinity on the absorption coefficient of water at visible wavelengths. A goal of this paper is to determine if a linear temperature slope Ψ_T and salinity slope Ψ_S exist so that the absorption coefficient of water can be given as

$$\alpha_w(\lambda, T, S) = \alpha_w(\lambda, T_r, 0) + \Psi_T(T - T_r) + \Psi_S S, \quad (1)$$

where T is the temperature, T_r is a reference temperature, and S is the salinity. Equation (1) is simply a Taylor series of first order based on temperature and salinity. We also investigate the possibility of a constant temperature dependence at visible wavelengths of the order of $0.001 \text{ m}^{-1}/^{\circ}\text{C}$ as has been reported by other investigators.^{1,4,5} As a check for possible interactions between temperature and salinity we look for differences in the temperature dependence between pure and saline water solutions. Finally, we estimate the magnitude of Ψ_T using a series of Gaussians that are fit to the absorption spectrum.

2. Background

To understand why temperature and salinity should be expected to affect the absorption coefficient of water we review the molecular structure of liquid water and its role in determining the absorption coefficient.

The water molecule has a polar arrangement that is responsible for many of its unusual properties. The polar nature of water allows hydrogen bonds between water molecules to form dimers, trimers, and larger clusters.^{3,16} The strength of the hydro-

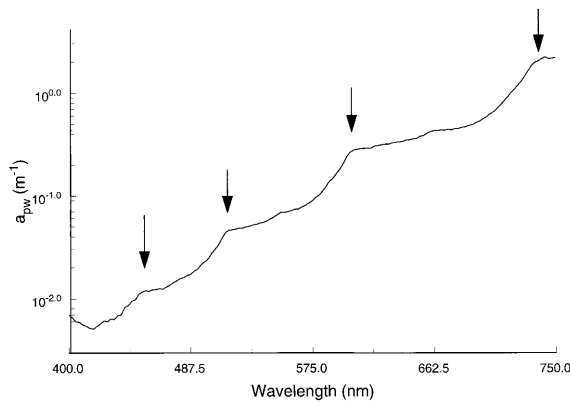


Fig. 2. Absorption coefficient of pure water as measured by Pope.¹⁸ The arrows point to the major absorption shoulders in the visible and the first absorption peak in the near infrared. Lesser absorption shoulders also exist at 555 and 665 nm.

gen bonds is low enough that thermal motion tends to break the clusters apart and thus the number and size of the clusters are dependent on temperature. The addition of ions to water causes larger, more tightly bound clusters, in which the ions are surrounded by a loose outer shell of water molecules.¹⁷ Both temperature and salinity therefore are expected to affect the molecular structure of water, which in turn affects the absorption properties of the water.

When light of wavelengths longer than 450 nm is absorbed, the energy is transferred to one or more of the vibrational modes of the O–H bond. The primary vibrational modes of liquid water are in the infrared at 3049 nm (symmetric stretch), 6079 nm (bend), and 2865 nm (asymmetric stretch).³³ Higher overtones of the vibrational modes can be seen as peaks and shoulders in the absorption spectrum of the visible region of the spectrum (Fig. 2). As the water molecules form hydrogen bonds with each other the O–H vibrational frequencies are shifted to longer wavelengths. As the temperature decreases the number of hydrogen-bonded molecules increases, which causes the absorption peaks to shift to longer wavelengths.

Light absorption at wavelengths in the ultraviolet is attributed to an electronic transition within the water molecule itself. The peak in the ultraviolet absorption occurs at 147 nm and absorption in the near ultraviolet represents the tail of that absorption maximum.¹⁹ At wavelengths near 400 nm the absorbed energy may go toward the electronic transition or vibrational mode, and it is therefore necessary to consider how the ultraviolet spectrum changes with temperature. There is a dearth of high-quality absorption-spectrum measurements of water in the ultraviolet with even fewer measurements of the temperature dependence.²⁰ The results of Halmann and Platzner²⁰ indicate that the ultraviolet absorption can change by as much as 4% at a reference temperature of 20° for every degree change in water temperature. In the blue portion of the spectrum an expected absorption coefficient^{18,21} of 0.01 m^{-1} would

Table 1. Wavelengths at which the Absorption Coefficient was Measured^a

Wavelength	ac-9	ac-9	a-3
412	X	X	
440	X	X	
488	X	X	
510		X	
520	X		
532	X	X	
555		X	
560	X		
650	X	X	
676	X	X	
715		X	
750	X		
850			X
900			X
975			X

^aThe potential error in the central wavelength of these filters is ± 2 nm. Wavelength selection was driven by the field applications of the instruments.

then result in a temperature dependence of less than $0.0004 \text{ m}^{-1}/^\circ\text{C}$.

3. Methods

Measurements of the absorption coefficient were made at discrete wavelengths in the visible and the near infrared using two 25-cm-path-length WETLabs ac-9's and a 10-cm-path-length WETLabs a-3 (three-wavelength-absorption meter).²² Temperature and salinity were measured with a SeaBird Electronics SBE-25 CTD. The data streams from the instruments were combined using a WETLabs Modular Ocean Data and Power System, and the combined data were archived on a computer. A time stamp from the Modular Ocean Data and Power System allowed the data streams to be merged based on time, which provided a single merged data file.

The wavelengths used in each of the WETLabs instruments were determined by selection of 10-nm-bandpass interference filters. The wavelengths used in the three instruments are given in Table 1. The selection of wavelengths provides good representation of the blue and green portions of the visible spectrum as well as a few wavelengths in the far-red and near-infrared regions. The 750- and 975-nm portions are near the central wavelengths of two of the higher-order vibrational overtones in the near infrared. Although we chose to use field instruments for this experiment, the results relate to the basic nature of water and not the performance of these instruments.

A. Laboratory Temperature Measurements

The plumbing configuration used for the temperature dependence test is shown in Fig. 3. A reverse-osmosis water system was used as the water source. The water from the reverse-osmosis system was then filtered with a $0.2\text{-}\mu\text{m}$ polishing filter before being passed to the temperature-control region. To con-

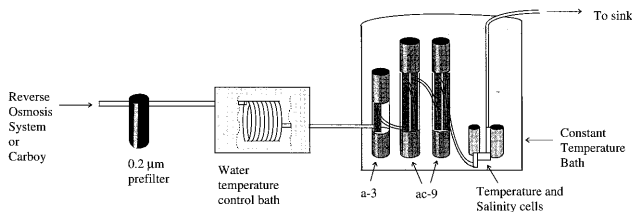


Fig. 3. Schematic diagram of the plumbing used for this experiment.

control the temperature the water was fed through a long length of tubing that was immersed in a water bath. The clean water temperature was varied by changing the temperature of the water bath. After passing through the temperature-control bath the water was sent to the instruments. The flow tubes of the a-3 and the ac-9's were plumbed in series along with the temperature and conductivity sensors of the CTD. Downstream from the conductivity cell outlet a valve was installed to provide backpressure to prevent the formation of bubbles in the tubing. The water-flow rate through the system was adjusted to approximately 2 L/min.

The internal temperature of the optical instruments is monitored to allow for temperature compensation of the electronics. To remove any residual electronic temperature dependence we stabilized the internal temperature of the instruments by placing them in a constant-temperature bath. The bath maintained the stability of the internal temperature to within 1 °C throughout the test. By keeping the electronics at a constant temperature, we ensured that small errors in the temperature compensation of the electronics do not affect the results of this study.

For the study of the influence of temperature on absorption measurements, data at a single temperature were collected over a 100-second period. When the data were merged it was necessary to account for the time lag for water to reach the different instruments. At the 2-L/min flow rate there was a 12.5-s difference between the time a parcel of water reached the first instrument and when it reached the last instrument. There occasionally was a sharp temperature gradient between water from the cooling coils and residual water left in the lines between runs. This temperature gradient could be observed in at least one channel of each instrument and was used to check the time alignment of the data set. Because the water temperature could vary by a few tenths of a degree during a measurement run, the temperature values were plotted as a function of time to determine a time period in which the temperature had the least variability. A subset of at least 12 s of data was collected from the time period with a nearly constant temperature, and the absorption and temperature records were averaged over this subset to provide a single data point with a standard deviation. A complete series of data points consisted of such measurements made at eight temperatures between 15 and 30 °C. The lower temperature limit was de-

termined by our ability to cool the warm (~30 °C) water from the reverse-osmosis water system. A linear least-squares regression was fit to each series of data to provide a slope of the absorption coefficient versus temperature for each wavelength. Five complete series of data and the slopes have been collected to provide an average value of the slopes with a standard deviation.

B. Laboratory Salinity Measurements

For tests of the absorption-coefficient dependence on salinity we used the reverse-osmosis water system as a source of water and combined the water with either NaCl or aquarium salts (Coralife scientific grade marine salt), referred to as artificial seawater in this paper. A 20-L polycarbonate carboy was filled with clean water, and salts were added in incremental portions to provide a wide range of salinities. The carboy was pressurized to 10 psi with nitrogen gas. The water from the carboy entered an activated charcoal filter to remove organics and then was passed through the 0.2- μm -pore-size polishing filter and the remainder of the system previously described. A collection carboy was added to allow the same water to be used in all the measurements. By collecting the water we were able to vary the temperature while maintaining a constant salinity. For salinity dependence measurements the collection carboy helped to ensure that the temperature of the saline solution was nearly constant throughout the experiment. Temperature variability throughout an experiment was held to less than 1 °C to minimize the possibility of temperature changes being interpreted as salinity effects. To reduce further the possible temperature effects the measured absorption coefficients were corrected to the mean temperature of each experiment (~21 °C) by means of the previously determined temperature corrections.

The salinity measurements were made over a longer time period to ensure that there was a complete change of water within the system. The temperature and salinity were plotted to ensure the selection of a time period when the two parameters were stable. A subset of the total data set was again used to provide a single data point.

C. Field Measurements

Field measurements using the ac-9's were used to verify the laboratory results. In the field the ac-9's, the SBE-25 CTD, and the Modular Ocean Data and Power System were combined on a free-falling platform for profiling. In some instances we installed a 0.2- μm -pore-size prefilter at the intake of the absorption flow tube of one ac-9. The filter allows us to measure the absorption of the dissolved component directly and allows us to observe changes in the absorption coefficient independent of the influence of particulate absorption.

In the field the absorption and attenuation meters were calibrated with water from a Barnstead nanopure water system. The water was collected in a 20-l polycarbonate carboy. The carboy was then at-

Table 2. Linear Slopes of the Temperature Dependence of the Absorption Coefficient Measured in the Laboratory^a

Wavelength	Ψ_T , Pure Water	Standard Deviation, Pure Water	Ψ_T , Saltwater	Standard Deviation, Saltwater
412	0.0001	0.0003	0.0003	0.0003
440	0.0000	0.0002	0.0002	0.0002
488	0.0000	0.0002	0.0001	0.0002
510	0.0002	0.0001	0.0003	0.0001
520	0.0001	0.0002	0.0002	0.0002
532	0.0001	0.0002	0.0001	0.0002
555	0.0001	0.0001	0.0002	0.0002
560	0.0000	0.0002	0.0000	0.0002
650	-0.0001	0.0001	-0.0001	0.0001
676	-0.0001	0.0001	-0.0001	0.0002
715	0.0029	0.0001	0.0027	0.0001
750	0.0107	0.0003	0.0106	0.0005
850	-0.0065	0.0001	-0.0068	0.0001
900	-0.0088	0.0001	-0.0090	0.0002
975	0.2272	0.0028	0.2273	0.0009

^aFor pure water the results of five tests are combined. The results of two tests were combined for the saltwater results. The absorption and attenuation meter results have been pooled together as well as pooling the common wavelengths between instruments. The standard deviations of the pooled values are provided.

tached to an ac-9 flow tube with Teflon tubing. A valve was placed on the outlet of the flow tube to provide backpressure. The carboy was then pressurized to 10 psi with a tank of dry nitrogen, and the valve was adjusted to provide a flow rate of approximately 1.5 L/min. The data were recorded for the pure water and used as a calibration blank for the instruments. The temperature of the calibration water was also recorded.

When the pure-water calibrations are applied to the ac-9's, the output of the instruments is the total absorption minus the absorption of the reference medium (i.e., pure water at a given temperature). An error proportional to the scattering coefficient also exists in the measured absorption value:

$$a_m = a_t - a_{wr} + \epsilon b, \tag{2}$$

$$a_t = a_p + a_d + a_w, \tag{3}$$

where a_m is the measured absorption coefficient, a_t is the total absorption coefficient, a_p is the absorption coefficient of the particulate matter, a_d is the absorption coefficient of the dissolved material, a_{wr} is the absorption coefficient of the reference water, a_w is the absorption coefficient of the water, b is the scattering coefficient, and ϵb is the scattering error. It is important to remember that a_{wr} is equal to a_w at only one specific temperature and salinity. Thus the measured absorption coefficient can be written as

$$a_m = a_p + a_d + (a_w - a_{wr}) + \epsilon b. \tag{4}$$

When a 0.2- μm filter is placed on the intake the measured dissolved absorption a_{md} is

$$a_{md} = a_d + (a_w - a_{wr}). \tag{5}$$

In Eq. (5) we have assumed that the scattering by particles passing through the 0.2- μm filter is negligible. Our experience with measurements taken

with filters on the absorption and attenuation sides indicates that, once temperature and salinity effects are accounted for, there is negligible difference between the two measurements, which indicates that this is a reasonable assumption. If there were significant scattering by materials passing through the filter then the absorption at each wavelength would be a factor of ϵb too high. Being able to remove the particulate contribution to the measured absorption coefficient makes it easier to study the effects of temperature and salinity on measurements made in the field.

4. Results of Laboratory Measurements

A. Temperature Measurements

In the laboratory we were able to remove the particulate and dissolved materials, which allowed us to study the changes in absorption that were due to water alone. We were also able to maintain the instruments at a constant temperature, which removes possible errors in the absorption measurements that are due to slight errors in the internal temperature compensation of the instrumentation. We are thus capable of confidently resolving slopes greater than $0.0004 \text{ m}^{-1}/^\circ\text{C}$. The results of five temperature-dependence tests on pure water and two on salt water are shown in Table 2. The results shown in Table 2 combine the common wavelengths of the two ac-9's and pool the absorption and attenuation measurements. We were unable to provide the full range of temperatures expected in the ocean; however, previous results^{6,8} indicate that the linear relationship holds down to lower temperatures.

It may be expected that the attenuation measurements have a different temperature dependence because the measurements would include the changes in the scattering coefficient with temperature. Morel² carried out a thorough analysis of the scattering

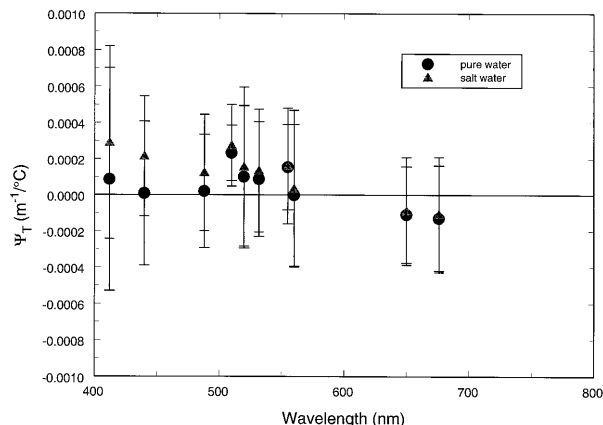


Fig. 4. Measured temperature slopes (Ψ_T) in the visible. The error bars represent ± 2 standard deviations of the measurements. There is no significant difference between the Ψ_T values for pure and saline water.

of pure and salt water based on the Einstein–Smoluchowski equation. From his results it can be seen that the scattering coefficient is directly proportional to temperature and indirectly related to temperature through the index of refraction and isothermal compressibility. Using Morel’s results Buiteveld *et al.*¹ performed an analysis of the effect of temperature on the scattering coefficient. Their study indicated that between 15 and 30 °C the scattering coefficient decreased by 2.4%, which translates into a maximum temperature dependence of the scattering coefficient of the order of $-1 \times 10^{-5} \text{ m}^{-1}/^\circ\text{C}$, which is insignificant compared to our observations of the temperature effect on absorption. Since the change in the scattering coefficient with temperature is negligible the change in the attenuation coefficient with temperature represents the change in the absorption contribution to the attenuation. Thus the change in the attenuation and absorption coefficients should be the same.

Our measured slopes of attenuation versus temperature were between 0.0004 and 0.0001 $\text{m}^{-1}/^\circ\text{C}$ lower than the absorption versus temperature slopes at the same wavelength. In no case, however, was there a statistically significant difference between the absorption slope and attenuation slope. Since there was no evidence that the two measurements should be treated separately we chose to combine the measurements.

Our results indicate that for measured wavelengths shorter than 700 nm the only wavelength region in which there is a possibly statistically significant temperature dependence is that at 510 nm (Fig. 4). The possible temperature dependence at 510 nm is expected because this wavelength corresponds to the peak of an overtone of the O–H vibrational frequency. Even if the results at 510 nm are statistically significant, the very small magnitude of the results makes the temperature dependence of little practical consequence. The absorption coefficient for wavelengths around 610 nm is also expected

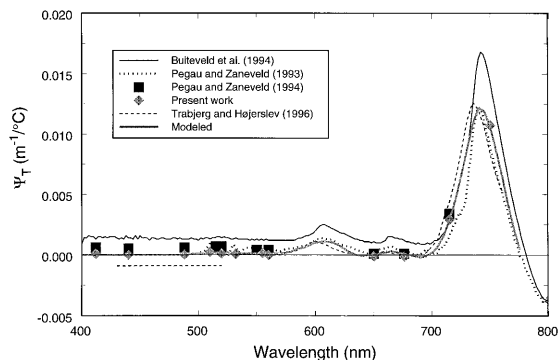


Fig. 5. Compilation of estimates of Ψ_T . In the visible there is a bias of 0.0011 between our measurements and those of Buiteveld *et al.* In regions of the peaks, some of the difference between the measurements can be due to errors in wavelength. When the peaks of Ψ_T are aligned the estimates are more consistent. Included with the measured values is a curve representing an estimate of Ψ_T based on the Gaussians fit to the absorption spectrum. The constant values of Ψ_T (0.003,⁴ -0.0015) reported in the blue and green portions of the spectrum are not provided in this plot.

to have a significant temperature dependence, but no measurements were made in this wavelength region. For wavelengths longer than 700 nm all the measured wavelength bands had a statistically and practically significant temperature dependence.

The results from this study are combined with the limited number of previous results^{1,5,7,9} and displayed in Fig. 5. Figure 5 does not display the spectrally constant temperature dependence in the blue–green portion of the spectrum that is discussed in earlier studies.^{4,5} The results of our study agree well with our preliminary data.⁹ We show slightly higher temperature dependencies at 715 and 750 nm than our 1993 study⁷ but it agrees well with the earlier results at shorter wavelengths. There is a bias of $0.0011 \text{ m}^{-1}/^\circ\text{C}$ throughout the visible region between our results and those of Buiteveld *et al.*¹ There is also a large difference in the magnitude of the peak temperature dependence in the near infrared between Buiteveld *et al.*¹ and other studies.^{5,6} The results reported in a recent paper by Trabjerg and Højerslev,⁵ which is that there is a $\Psi_T = -0.0009 \text{ m}^{-1}/^\circ\text{C}$ in the blue–green portion of the spectrum, did not reproduce in our results, most likely because our instrumentation does not allow for the long settling times that were required to obtain their result. There is good agreement in the magnitude of Ψ_T between the results of Trabjerg and Højerslev in the yellow and red portions of the spectrum compared with this and previous studies. The largest difference is in the location of the peak in the temperature dependence with our studies indicating that the peak is at 740 nm versus 735 nm as reported by Trabjerg and Højerslev. Near the absorption peak at 740 nm Ψ_T changes rapidly, thus small errors in wavelength can create large differences in estimates of Ψ_T . For example, at 715 nm the ± 2 -nm uncertainty in the central wavelength of an interference filter creates

Table 3. Estimates of Ψ_T Calculated Based on Ψ_T as a Percentage of the Magnitude of the Gaussian Fit to the Absorption Spectrum of Pure Water^a

λ	Ψ_T	λ	Ψ_T	λ	Ψ_T	M	σ	λ_c	M_T
500	0.0001	585	0.0004	670	0.0002	.18	18	453	0.0045
505	0.0001	590	0.0006	675	0.0001	.17	15	485	0.002
510	0.0002	595	0.0008	680	<0.0001	.52	14	517	0.0045
515	0.0002	600	0.0010	685	-0.0001	1.4	20	558	0.002
520	0.0002	605	0.0011	690	-0.0002	4.6	17.5	610	0.0045
525	0.0002	610	0.0011	695	-0.0001	2.1	15	638	-0.004
530	0.0001	615	0.0010	700	0.0002	4.3	17	661	0.002
535	0.0001	620	0.0008	705	0.0007	9.6	22	697	-0.001
540	0.0001	625	0.0005	710	0.0016	1.6	6	740	0.0045
545	0.0001	630	0.0002	715	0.0029	34	18	744	0.0062
550	0.0001	635	<0.0001	720	0.0045	18	20	775	-0.001
555	0.0001	640	-0.0001	725	0.0065	42	25	795	-0.001
560	0.0001	645	<0.0001	730	0.0087				
565	0.0002	650	<0.0001	735	0.0108				
570	0.0002	655	0.0001	740	0.0122				
575	0.0002	660	0.0002	745	0.0120				
580	0.0003	665	0.0002	750	0.0106				

^aThe magnitude M , width σ , central wavelength λ_c , and temperature percentage multiplier M_T for the fit to the water absorption curve are also provided for this wavelength range. The value of Ψ_T is given by $\Psi_T = \sum \{M_T(M/\sigma)\exp -[(\lambda - \lambda_c)^2/2\sigma^2]\}$. Outside of the near infrared the only wavelengths with a temperature dependence of the order of $0.001 \text{ m}^{-1}/^\circ\text{C}$ are near 610 nm. From 400 to 500 nm the value of Ψ_T is $<0.0001 \text{ m}^{-1}/^\circ\text{C}$.

a range of possible temperature slopes of $0.0023\text{--}0.0035 \text{ m}^{-1}/^\circ\text{C}$ depending on the actual central wavelength.

B. Temperature Model

A more complete temperature dependence spectrum can be estimated from a modeled absorption spectrum of water. The absorption spectrum can be simulated by a series of Gaussian curves representing the absorption at the O–H vibrational overtones. It is expected that a continuum of separate Gaussians for each configuration of water molecules would be necessary to represent the absorption spectrum properly. However, we found that a good fit to a measured absorption spectrum could be achieved with a single Gaussian for overtones shorter than 600 nm and a pair of Gaussians for each of the vibrational overtones at longer wavelengths. The pair of Gaussians consisted of one at the absorption shoulder and a second Gaussian at a longer wavelength. The absorption peak at 740 nm required two pairs of Gaussians for a good fit.

To make the temperature dependence spectrum conform to the present and earlier⁷ measurements required that the magnitude of the shorter-wavelength Gaussian of the pair have a positive dependence on temperature, and the magnitude of the longer-wavelength Gaussian have a negative temperature dependence. This is consistent with the concept that the shorter-wavelength Gaussian represented absorption by individual molecules and clusters of a few water molecules. At higher temperatures more molecules would be in smaller clusters, and thus the absorption by these molecules would increase with temperature. In contrast, the absorption at the longer-wavelength Gaussian would represent absorption by large clusters of water molecules. The num-

ber of the larger clusters would decrease with increasing temperature and the absorption would have a negative temperature dependence.

Based on the temperature dependencies measured in this study and in our earlier study⁷ in the red and near-infrared portions of the spectrum we can model the temperature dependence by using the Gaussian curves fit to the absorption spectrum. The temperature dependence of the Gaussians with peak values in the region of absorption peaks and larger shoulders is approximately $0.5\%/^\circ\text{C}$ of absorption at 20°C . The smaller absorption shoulders that can be seen in Fig. 2 at 555 nm and 665 nm would have a smaller temperature dependence. The Gaussian curves fit in these shoulders are multiplied by 0.2% to arrive at the temperature dependence. The small absorption combined with a small temperature dependence prevents us from observing a peak at 555 nm. The measured peaks in the temperature dependence spectrum can be recreated well by use of the Gaussian curves. The fitted values are shown in Fig. 5 and in Table 3. We estimate that the temperature dependencies obtained from the Gaussian curves are accurate to within $\pm 0.0004 \text{ m}^{-1}/^\circ\text{C}$ throughout the visible portion of the spectrum.

C. Salinity Measurements

Measurements were made on artificial seawater to determine if the absorption coefficient of water is dependent on salinity. During the first set of measurements organic contaminants in the artificial seawater obscured any possible salinity dependence in the visible portion of the spectrum. The absorption by organics was evident as an exponentially increasing absorption towards shorter wavelengths, which could be removed by filtering with an activated charcoal filter. The values of Ψ_S from the first ex-

Table 4. Slopes of the Absorption Coefficient versus Salinity Based on Linear Regression Analysis

Wavelength	Ψ_s Attenuation	Standard Deviation Attenuation
412	0.00012	0.00005
440	-0.00002	0.00002
488	-0.00002	0.00002
510	-0.00002	0.00003
532	-0.00003	0.00006
555	-0.00003	0.00003
650	0.00000	0.00003
676	-0.00002	0.00002
715	-0.00027	0.00006
750	0.00064	0.00003

^aA constant of 0.00005 has been added to each measured Ψ_s to correct for changes in the primary reflectance at the instrument windows that are due to changes in salinity.

periment for wavelengths longer than 650 nm are included in the results provided in Table 4. At these longer wavelengths the absorption by dissolved organics is negligible in its effects on the determination of salinity slope.

A second set of measurements was made with an activated charcoal filter added to remove organics. Measurements were made on NaCl solutions. Results are provided in Table 4 for which the NaCl concentration is provided as an equivalent salinity. For wavelengths above 650 nm there was no statistical difference between the NaCl solution and the artificial seawater even though the NaCl solution lacks ions that are present in the artificial seawater. Throughout most of the visible wavelengths the salinity slope is less than $0.00015 \text{ m}^{-1}/\text{PSU}$. For seawater samples of 35 PSU referenced to fresh water a slope of $0.00015 \text{ m}^{-1}/\text{PSU}$ represents a 0.005-m^{-1} error. Unlike the temperature results, Table 4 does not pool the absorption and attenuation measurements. As can be seen in Fig. 6, the attenuation coefficient was found to be linearly dependent on salinity. The absorption measurement was also dependent on salinity, however, the salinity slopes for the two measurements were found to be statistically

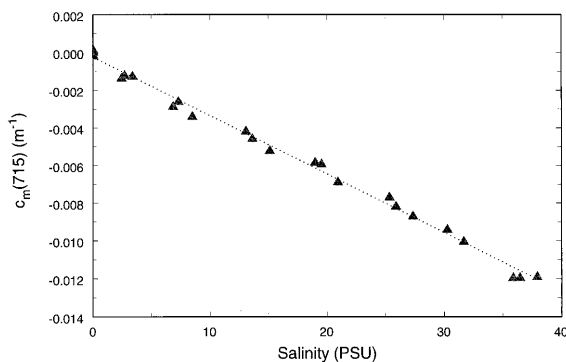


Fig. 6. Attenuation coefficient at 715 nm as a function of salinity. This figure illustrates the linear dependence of the attenuation coefficient on salinity.

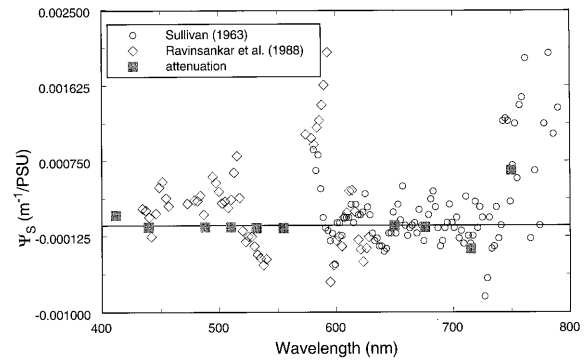


Fig. 7. Our salinity results combined with the results of previous investigations.

different because of instrumental effects. The reason for the difference is presented later in this paper. Our results are presented together with earlier results^{10,11} in Fig. 7. From this figure it can be seen that our results lie well within the previous results. After accounting for instrumental effects the salinity slope in the visible region as measured with the attenuation meter is not significantly different from zero except at 412 nm.

The effect of reduced primary water-glass reflectance at the instrument windows with increasing salinity must be accounted for in the salinity measurements. The change in the index of refraction of water with salinity is approximately five times greater than that for temperature given the range of temperature and salinities used in this experiment.²³ The index of refraction changes in a linear manner over the measured salinity range.²³ The index-of-refraction effect could add a linear dependence on salinity that is not related to changes in the absorption properties of water. Calculation of change in the reflectance at the fused quartz windows indicates that a change of salinities from 0 to 35 PSU causes the instruments to read 0.0017 m^{-1} ($\Psi_s = -0.00005$) lower. The research of Trabjerg and Højerslev⁵ shows that the change in index of refraction that is due to temperature has an insignificant impact on the results. For the salinity measurements the change in the transmission of higher-order reflections is important in the absorption meter because of the large portion of light reflected by the diffuser. Modeling of this effect requires knowledge of the bidirectional reflectance distribution function and transmissivity of the filter. Because we lack this information we cannot fully correct the absorption measurements from instrumental salinity effects and therefore do not present the absorption-meter data. In general, the measured absorption Ψ_s values were $0.00015 \text{ m}^{-1}/\text{PSU}$ higher than the attenuation values because of the multiple reflections in the ac-9. The changes in reflectance that are due to salinity must be accounted for when one uses an analyzing spectrophotometer or ac-9 data. The slopes given in Table 4 are inherent to water and are not meant to be used as instrumental corrections.

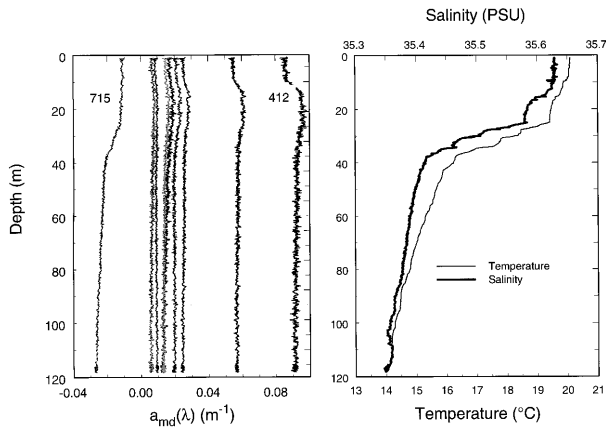


Fig. 8. Profile of absorption of water passed through a 0.2- μm filter and the physical parameters of temperature and salinity. Wavelength decreases from 715 nm at the left to 412 nm at the right. At 412 and 440 nm there is evidence of variability in the concentration of dissolved organics. Only at 715 nm is there evidence of changes in the measured absorption related to the physical parameters.

Changes in the scattering coefficient with increasing salinity can also influence our measurements. Morel² found that there was a 30% increase in the scattering coefficient between fresh and saline water. The increase in scattering tended to cause the attenuation measurement to have a more positive Ψ_S than can be attributed to changes in absorption alone. This effect is largest at 412 nm ($\sim 0.0014 \text{ m}^{-1}$ or $\Psi_S = 0.00005 \text{ m}^{-1}/\text{PSU}$) but is negligible for most of the visible wavelengths. The remainder can be the result of absorption by a salt or a shift in the ultraviolet absorption peak toward longer wavelengths. Without measurements at shorter wavelengths it is not possible to isolate the cause of the change in Ψ_S at 412 nm.

D. Field Measurements

Although laboratory research is necessary to understand how the absorption by water is affected by temperature and salinity, it is important to verify that the laboratory results make sense when applied to field measurements. During various cruises we collected a large number of measurements of total absorption coefficients and dissolved-component absorption coefficients. The results presented in this paper were obtained during a December 1995 cruise in the Gulf of California; similar results were found during other cruises in a variety of locations. We use the dissolved-absorption results to discuss the dependence of field measurements on temperature and salinity for a couple of reasons. First, the absorption by particulate material was removed so that there was one less confounding factor. Second, the absorption by dissolved materials was low in the near-infrared portion of the spectrum where, based on the laboratory results, we expected the largest dependence on temperature and salinity.

A vertical profile of the measured absorption by dissolved materials is shown in Fig. 8. Although the

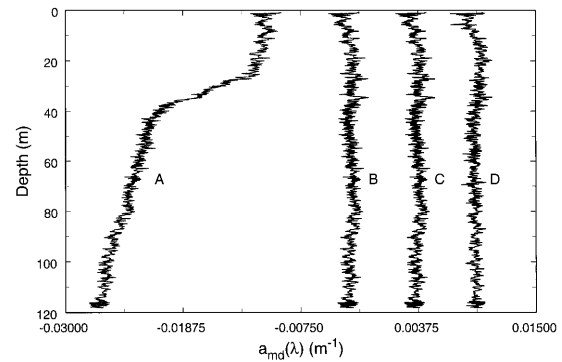


Fig. 9. Laboratory values of Ψ_T and Ψ_S applied to field measurements of $a_{md}(715)$ for water that has been passed through a 0.2- μm filter. Curve D is $a_{md}(650)$ and is expected to be similar in shape as well as slightly greater in magnitude than $a_{md}(715)$. Curve A is the measured value of $a_{md}(715)$. Curve B is $a_{md}(715)$ with the temperature correction applied. Note that curve B is similar to curve D but the magnitude is less than zero. Applying the salinity correction to the temperature corrected $a_{md}(715)$ gives curve C. Curve C is of the same shape and magnitude for the dissolved component, given curve D as a reference.

absorption by dissolved substances is not constant throughout the profile, the only wavelength at which the absorption coefficient seems to have an obvious correlation with temperature or salinity is 715 nm. A closer look at the measured absorption in the red and the infrared shows the dependence of the absorption coefficient at 715 nm on temperature and salinity. Figure 9 illustrates the effect of applying the laboratory temperature and salinity corrections to $a_{md}(715)$. It can be seen that $a_{md}(650)$ was nearly constant with depth. There is little expected difference between $a_d(715)$ and $a_d(650)$, so we expect the two wavelengths to have similar profiles. The $a_{md}(715)$, however, has a much different vertical profile than $a_{md}(650)$ (profiles A and D in Fig. 9). The vertical shape of the measured profile of $a_d(715)$ changes to that of $a_d(650)$ when the temperature correction is applied (profile B, Fig. 9). Even after the temperature correction is applied the measured value of $a_d(715)$ remains negative, implying that the water is clearer than the calibration water. Because the range of salinity is small over this profile the salinity correction merely adds a constant related to the difference in absorption between the pure and saline waters. Once the salinity correction given in Table 4 is applied, the $a_d(715)$ value becomes positive and slightly less than $a_d(650)$ in magnitude as would be expected for measurements of dissolved materials (profile C, Fig. 9).

If the temperature dependence in the visible region was of the order of $0.001 \text{ m}^{-1}/^\circ\text{C}$ as has been suggested,^{1,4,5} we should be able to see evidence of its effect on the measured profiles. We occasionally find vertical profiles of dissolved material absorption that are constant with depth even though a thermal structure may exist. Equation (5) shows that if a_{md} is constant, $\Delta a_d = -\Delta(a_w - a_{wr})$ for the entire profile. The application of a temperature correction of ± 0.001

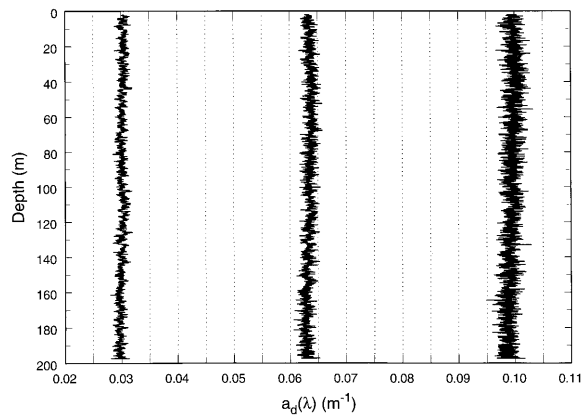


Fig. 10. From left to right are the measured values of absorption by the dissolved component at 488, 440, and 412 nm. The water temperature changed by 5° over the depth of the profile. If the proposed constant temperature dependence of the order of 0.001 m⁻¹/°C existed, a change in the concentration of dissolved matter can compensate for the expected change in water absorption. However, a change in absorption by dissolved materials cannot match the expected change in water absorption at all three wavelengths. A corresponding change in the spectral slope of the yellow matter would also need to occur to provide these results. Since all three wavelengths exhibit the same vertical profile it is unlikely that a constant value of Ψ_T exists in the visible.

m⁻¹/°C would provide a spectrally constant value of $\Delta(a_w - a_{wr})$ and hence a spectrally constant Δa_d .

For the case in Fig. 10 there was a 5° change in water temperature over the profile depth. If the measured $a_d(488)$ was constant because changes in the concentration of the dissolved organics compensated for changes in the water absorption there would be a $\Delta a_d(488) = 0.005 \text{ m}^{-1}$ from the top of the profile to the bottom unless there was a corresponding change in the exponential slope with concentration. Assuming that dissolved absorption can be modeled with an exponential function with 488 nm as a reference wavelength²⁴ and that there is a constant slope of -0.015 (see Fig. 10), then

$$a_d(\lambda) = a_d(488) * \exp[-0.015 * (\lambda - 488)], \quad (6)$$

and then the expected $\Delta a_d(412)$ would be 0.016 m⁻¹. Subtracting the constant temperature dependence of 0.005 m⁻¹ leaves an expected change of 0.011 m⁻¹, which is not evident in Fig. 10. Using an exponential model of the absorption spectrum of dissolved materials it is not possible to explain the results in Fig. 10 as a change in the slope coinciding with a change in concentration. Thus a constant temperature dependence of the order of 0.001 m⁻¹/°C in the visible portion of the spectrum is not evident in the field measurements.

In cases in which the absorption by dissolved materials does not vary with depth, the coefficient of the temperature dependence can be estimated by regressing the measured $a_d(\lambda)$ against temperature. The temperature variation in a typical profile is most often <10°. Combined with the small expected dependence of the absorption coefficient on tempera-

Table 5. Slopes of Linear Regression of Dissolved Absorption Coefficients Measured in the Ocean versus Temperature^a

Wavelength	Slope
412	0.0003
440	0.0002
488	0.0001
510	0.0004
555	0.0005
650	-0.0002
676	0.0001
715	0.0027

^aThe data used are those presented in Fig. 10, where the dissolved material absorption appears to be constant with depth. The up and down casts have been evaluated to ensure that the internal temperature compensation affected the measurement by less than 0.002 m⁻¹. Although this is a small number it still represents a possible slope error of 0.0004 m⁻¹/°C. It is also possible that there is some vertical variability in dissolved material concentration, which would affect the results most strongly at the shorter wavelengths.

ture, the expected change in magnitude is in the third decimal place of the measurements. Errors in the temperature compensation of the electronics can cause the measured absorption coefficients to vary at this level, making it difficult to separate the two effects. A check on the quality of the electronic temperature compensation can be achieved by looking at both the up and down portions of a cast. Wavelengths with imperfect temperature calibrations will have a hysteresis in the profile related to the large thermal mass of the instrument. By performing a linear regression of the measured dissolved absorption against the temperature for the profile provided in Fig. 10 we have estimated the magnitude of the temperature dependence for the wavelengths measured. The results of the regression analysis are provided in Table 5. With the exception of 555 nm the field results are in excellent agreement with the laboratory tests. The difference at 555 nm is attributed to instrumental-temperature-compensation errors.

5. Conclusions

Our results verify that linear slopes can be used to correct the absorption coefficient for changes in both temperature and salinity encountered in natural waters. The temperature dependence was not statistically different for pure and saline water, indicating that it is possible to ignore interaction terms of temperature and salinity when making corrections to the absorption coefficient.

The effects of temperature appear to be restricted to near the central wavelengths of the overtones of the O-H vibrational frequencies. Neither our laboratory nor field data provides any evidence of the previously reported^{1,4,5} spectrally constant temperature dependence in the visible region. With the exception of wavelengths near 610 nm it would appear that the magnitude of Ψ_T is less than 0.001 m⁻¹/°C throughout the visible region of the spectrum. The measured temperature dependencies were modeled

with a series of Gaussians fit to the absorption spectrum. The Gaussians peaked in the regions of the major absorption shoulders, and the peaks had a temperature dependence of 0.5% of the magnitude of the Gaussian.

As was true with temperature, the only significant salinity dependence measured was in the near-infrared portion of the spectrum. The salinity dependence, however, was much less pronounced than the temperature dependence and not always in the same direction as temperature. This is the case at 715 nm at which increasing temperature increases the absorption coefficient, but increasing salinity decreases the absorption coefficient. Extrapolating this result into the visible region, we would expect the salinity dependence in the visible region to be negligible, as was confirmed by the salinity effect on the measured attenuation coefficients. The only measurement with a significant salinity dependence in the visible region was at 412 nm.

The degree of precision in the slopes that is necessary to compensate observed values is generally different for temperature and salinity. The temperature of the calibration or reference water is commonly within 10–15° of the water to be measured. A 0.0002-m⁻¹/°C error in the value of Ψ_T therefore becomes a 0.003-m⁻¹ error in the measured absorption value for a ΔT of 15°. However, the reference water usually has a salinity of 0 PSU, and seawater samples typically have a salinity of 35 PSU, which creates a 0.007-m⁻¹ measurement error for a 0.0002-m⁻¹/PSU error in the value of Ψ_S . When analyzing measurements it is also important to account for the changes in reflectance at the windows when referencing a seawater sample to pure water.

The result that the absorption coefficient of water is dependent on temperature and salinity is important to investigators who measure the optical properties of natural waters in the near infrared. For example, when the absorption coefficient at a wavelength in the near infrared is used for estimating the scattering error in a measurement,²⁵ it is important to account for the differences in temperature and salinity between the sample and the reference water. Variations in the optical properties of water can also account for baseline offsets that reportedly plague dissolved material absorption measurements.⁷ These baselines commonly are obtained from measurements in the near infrared where the effects of temperature and salinity are largest.

This research was supported by the Environmental Optics branch of the Office of Naval Research and by the National Aeronautics and Space Administration under grant NAGW-3580. We thank N. K. Højerslev and an anonymous reviewer for their comments, which have improved this manuscript.

References

1. H. Buiteveld, J. M. H. Hakvoort, and M. Donze, "The optical properties of pure water," in *Ocean Optics XII*, J. S. Jaffe, ed., Proc. SPIE **2258**, 174–183 (1994).
2. A. Morel, "Optical properties of pure water and pure sea wa-

- ter," in *Optical Aspects of Oceanography*, N. G. Jerlov and E. S. Nielsen, eds. (Academic, London, 1974), pp. 1–24.
3. D. H. Everett, "How much do we really know about water?" in *Water and Aqueous Solutions*, Vol. 37, G. W. Neilson and J. E. Enderby, eds. (Hilger, London, 1985), pp. 331–342.
4. N. K. Højerslev and I. Trabjerg, "A new perspective for remote sensing measurements of plankton pigments and water quality," Report 51 (University of Copenhagen, Institute of Physical Oceanography, Copenhagen, 1990).
5. I. Trabjerg and N. K. Højerslev, "Temperature influence on light absorption by fresh water and seawater in the visible and near-infrared spectrum," *Appl. Opt.* **35**, 2653–2658 (1996).
6. W. S. Pegau, J. S. Cleveland, W. Doss, C. D. Kennedy, R. A. Maffione, J. L. Mueller, R. Stone, C. C. Trees, A. D. Weidemann, W. H. Wells, and J. R. V. Zaneveld, "A comparison of methods for the measurement of the absorption coefficient in natural waters," *J. Geophys. Res.* **100**, 13,201–13,220 (1995).
7. W. S. Pegau and J. R. V. Zaneveld, "Temperature-dependent absorption of water in the red and near-infrared portions of the spectrum," *Limnol. Oceanogr.* **38**, 188–192 (1993).
8. S. A. Green and N. V. Blough, "Optical absorption and fluorescence properties of chromophoric dissolved organic matter in natural waters," *Limnol. Oceanogr.* **39**, 1903–1916 (1994).
9. W. S. Pegau and J. R. V. Zaneveld, "Temperature dependence of the absorption coefficient of pure water in the visible portion of the spectrum," in *Ocean Optics XII*, J. S. Jaffe, ed., Proc. SPIE **2258**, 597–604 (1994).
10. M. Ravisankar, A. T. Reghunath, K. Sathianandan, and V. P. N. Nampoori, "Effect of dissolved NaCl, MgCl₂, and Na₂SO₄ in seawater on the optical attenuation in the region from 430 to 630 nm," *Appl. Opt.* **27**, 3887–3894 (1988).
11. S. A. Sullivan, "Experimental study of the absorption in distilled water, artificial sea water, and heavy water in the visible region of the spectrum," *J. Opt. Soc. Am.* **53**, 962–968 (1963).
12. J. R. Collins, "Change in the infra-red absorption spectrum of water with temperature," *Phys. Rev.* **25**, 771–779 (1925).
13. W. Luck, "Beitrag zur Assoziation des flussigen Wassers. I. Die Temperaturabhängigkeit der Ultrarotbanden des Wassers," *Ber. Bunsenges. Physik. Chem.* **67**, 186–189 (1963).
14. W. C. Waggener, A. J. Weinberger, and R. W. Stoughton, "The absorption spectrum of H₂O and D₂O in the near infrared region as a function of temperature from –20° to 250 °C," Report ONRL-P-925 (Atomic Energy Commission, Washington, D.C., 1964).
15. J. Lin and C. W. Brown, "Near-IR spectroscopic measurement of seawater salinity," *Environ. Sci. Technol.* **27**, 1611–1615 (1993).
16. A. D. Buckingham, "The structure and properties of a water molecule," in *Water and Aqueous Solutions*, Vol. 1, G. W. Neilson and J. E. Enderby, eds. (Hilger, Bristol, 1986), pp. 1–10.
17. J. Dera, *Marine Physics* (Elsevier, Amsterdam, 1992).
18. R. M. Pope, "Optical absorption of pure water and seawater using the integrating cavity absorption meter," Ph.D. dissertation (Texas A&M College, College Station, Tex., 1993).
19. T. I. Quickenden and J. A. Irvin, "The ultraviolet absorption spectrum of liquid water," *J. Chem. Phys.* **72**, 4416–4428 (1980).
20. M. Halmann and I. Platzner, "Temperature dependence of absorption of liquid water in the far-ultraviolet region," *J. Phys. Chem.* **70**, 580–581 (1966).
21. L. P. Boivin, W. F. Davidson, R. S. Storey, D. Sinclair, and E. D. Earle, "Determination of the attenuation coefficients of visible and ultraviolet radiation in heavy water," *Appl. Opt.* **25**, 877–882 (1986).
22. C. Moore, "In situ, biochemical, oceanic, optical meters," *Sea Technol.* **35**, 10–16 (1994).

23. R. W. Austin and G. Halikas, "The index of refraction of seawater," Report SIO Reference 76-1 (Scripps Institution of Oceanography, San Diego, Calif., 1976).
24. C. S. Roesler, M. J. Perry, and K. L. Carder, "Modeling *in situ* phytoplankton absorption from total absorption spectra in productive inland marine waters," *Limnol. Oceanogr.* **34**, 1510–1523 (1989).
25. J. R. V. Zaneveld, J. C. Kitchen, and C. Moore, "The scattering error correction of reflecting-tube absorption meters," in *Ocean Optics XII*, J. S. Jaffe, ed., Proc. SPIE **2258**, 44–55 (1994).
26. K. S. Shifrin, *Physical Optics of Ocean Water* (American Institute of Physics, New York, 1988).
27. R. C. Smith and K. S. Baker, "Optical properties of the clearest natural waters (200–800 nm)," *Appl. Opt.* **20**, 177–184 (1981).
28. A. C. Tam and C. K. N. Patel, "Optical absorptions of light and heavy water by laser optoacoustic spectroscopy," *Appl. Opt.* **18**, 3348–3358 (1979).
29. W. M. Irvine and J. B. Pollack, "Infrared optical properties of water and ice spheres," *Icarus* **8**, 324–360 (1968).
30. M. R. Querry, D. M. Wieliczka, and D. J. Segelstein, "Water (H₂O)," in *Handbook of Optical Constants of Solids II*, E. D. Palik, ed. (Academic, New York, 1991), pp. 1059–1077.
31. M. R. Querry, P. G. Cary, and R. C. Waring, "Split-pulse laser method for measuring attenuation coefficients of transparent liquids: application to deionized filtered water in the visible region," *Appl. Opt.* **17**, 3587–3592 (1978).
32. G. M. Hale and M. R. Querry, "Optical constants of water in the 200-nm to 200- μ m wavelength region," *Appl. Opt.* **12**, 555–563 (1973).
33. J. B. Bayly, V. B. Kartha, and W. H. Stevens, "The absorption spectra of liquid phase H₂O, HDO and D₂O from 0.7 μ m to 10 μ m," *Infrared Phys.* **3**, 211–222 (1963).